Full Electrical Control of the Electron Spin Relaxation in GaAs Quantum Wells

A. Balocchi,[1] Q. H. Duong,[1] P. Renucci,[1] B. L. Liu,[2] C. Fontaine,[3] T. Amand,[1] D. Lagarde,[1] and X. Marie[1,*]

[1]*Université de Toulouse, INSA-CNRS-UPS, LPCNO, 135 avenue de Rangueil, 31077 Toulouse, France*

[2]*Beijing National Laboratory for Condensed Matter Physics, Institute of Physics, Chinese Academy of Sciences, P.O. Box 603, Beijing 100190, People's Republic of China*

[3]*LAAS, CNRS, Université de Toulouse; 7 avenue du Colonel Roche, F-31077 Toulouse, France*

(Received 27 July 2011; published 19 September 2011)

The electron spin dynamics in (111)-oriented GaAs/AlGaAs quantum wells is studied by time-resolved photoluminescence spectroscopy. By applying an external electric field of 50 kV/cm a two-order of magnitude increase of the spin relaxation time can be observed reaching values larger than 30 ns; this is a consequence of the electric field tuning of the spin-orbit conduction band splitting which can almost vanish when the Rashba term compensates exactly the Dresselhaus one. The measurements under a transverse magnetic field demonstrate that the electron spin relaxation time for the three space directions can be tuned simultaneously with the applied electric field.

DOI: 10.1103/PhysRevLett.107.136604 PACS numbers: 72.25.Fe, 72.25.Rb, 78.67.De

The control of electron spin in semiconductors for potential use in transport devices or quantum information applications has attracted a great deal of attention in recent years [1–3]. In 2D nanostructures made of III-V or II-VI semiconductors, the dominant loss of electron spin memory is related to the spin relaxation mechanism known as the Dyakonov-Perel (DP) mechanism [4,5]. In these materials, the absence of inversion symmetry and the spin-orbit (SO) coupling are responsible for the lifting of the degeneracy for spin $|1/2\rangle$ and $|-1/2\rangle$ electrons states in the conduction band (CB). This splitting plays a crucial role for the spin manipulation and spin transport phenomena [6,7]. As it depends strongly on the crystal and nanostructure symmetry [8–10], it can be efficiently tailored as explained below. The SO splitting can be viewed as the result of the action on the electron spin of an effective magnetic field whose amplitude and direction depend on the wave vector $\boldsymbol{k}$ of the electron. The electron spin will precess around this field with an effective, momentum dependent Larmor vector $\boldsymbol{\Omega}$ whose magnitude corresponds to the CB spin splitting. This effective magnetic field changes with time since the direction of the electron momentum varies due to electron collisions. As a consequence, spin precession around this field in the intervals between collisions gives rise to spin relaxation. In the usual case of frequent collisions, the relaxation time of an electron spin oriented along the direction i can be written [4] $(\tau_s^i)^{-1} = \langle\Omega_\perp^2\rangle\tau_p^*$, where $\langle\Omega_\perp^2\rangle$ is the mean square precession vector in the plane perpendicular to the direction i ($i = x, y, z$) and τ_p^* the electron momentum relaxation time. This yields the loss of the electron spin memory in a few tens or hundreds of picoseconds [11,12]. As the driving force in the DP spin relaxation is the SO splitting, its reduction is expected to lead to an increase of the spin relaxation time [13,14]. In bulk zinc-blende semiconductor, the bulk inversion asymmetry (BIA) spin splitting, also called Dresselhaus term, is determined by [1,8]:

$$\boldsymbol{\Omega}_{\mathrm{BIA}}^{\mathrm{3D}}(\boldsymbol{k}) = \frac{\gamma}{\hbar}[k_x(k_y^2 - k_z^2), k_y(k_z^2 - k_x^2), k_z(k_x^2 - k_y^2)], \quad (1)$$

where γ is the Dresselhaus coefficient and $\boldsymbol{k} = (k_x, k_y, k_z)$ the electron wave vector. In a quantum well (QW), where the momentum component along the growth axis $\mathbf{z}$ is quantized, the vector $\boldsymbol{\Omega}$ due to the BIA for the lowest electron subband is written as

$$\boldsymbol{\Omega}_{\mathrm{BIA}}(\boldsymbol{k}_\parallel) = \frac{\gamma}{\hbar}\langle k_z^2\rangle(-k_x, k_y, 0) \quad \text{if } \mathbf{z} \parallel [001], \quad (2a)$$

$$\boldsymbol{\Omega}_{\mathrm{BIA}}(\boldsymbol{k}_\parallel) = \frac{\gamma}{2\hbar}\langle k_z^2\rangle(0, 0, k_y) \quad \text{if } \mathbf{z} \parallel [110], \quad (2b)$$

$$\boldsymbol{\Omega}_{\mathrm{BIA}}(\boldsymbol{k}_\parallel) = \frac{2\gamma}{\hbar\sqrt{3}}\langle k_z^2\rangle(k_y, -k_x, 0) \quad \text{if } \mathbf{z} \parallel [111], \quad (2c)$$

where $\langle k_z^2\rangle$ is the averaged squared wave vector along the growth direction and $\boldsymbol{k}_\parallel$ is the in-plane wave vector. The weaker cubic terms in the Hamiltonian have been neglected here since $\langle k_z^2\rangle > k_x^2, k_y^2$; their influence will be discussed later in the Letter. If an external electric field is applied or an asymmetric doping, which generates a built-in electric field, is present in the structure, an additional contribution to the spin splitting appears, and is usually referred to as structural inversion asymmetry (SIA) or the Rashba effect [9,15–18]. For an electric field applied along the growth axis, this SIA term is written as

$$\boldsymbol{\Omega}_{\mathrm{SIA}}(\boldsymbol{k}_\parallel) = \frac{\alpha}{\hbar}(k_y, -k_x, 0), \quad (3)$$

where $\alpha = aE$ is the Rashba coefficient (E is the electric field amplitude and a is a positive constant). Note that the SIA vector is perpendicular to both the electron momentum and the electric field ($\boldsymbol{\Omega} \propto \boldsymbol{E} \times \boldsymbol{k}_\parallel$). As shown in Eqs. (2) and (3) both the BIA and SIA strengths can be

controlled [15]. The modification of the electron quantum confinement (through the well width L variation of the $\langle k_z^2 \rangle$ term, for instance [11]) allows the tuning of the BIA spin splitting, whereas the SIA term can be easily varied through the applied electric field amplitude.

For (001) quantum wells, the interplay of the BIA and SIA terms leads to an in-plane anisotropic CB spin splitting [Eqs. (2a) and (3)] [15,19–21]. By tuning the QW asymmetry, longer DP spin relaxation times along the in-plane [110] direction was demonstrated [22–25].

For (110) quantum wells, it turns out that the effective magnetic field due to the BIA term is oriented along the [110] growth direction [Eq. (2b)] [5]; if the electron spin S_z is also aligned along this direction, the DP spin relaxation mechanism is suppressed, leading to τ_s^z, as long as 20 ns for electron spins parallel to [110] [26,27]. This is not true for spins prepared in other directions due to strongly anisotropic spin relaxation in these (110) GaAs quantum wells [27–29].

In contrast to (100) and (110) QW, where the DP spin relaxation can vanish for one given spin direction, it can be suppressed in principle for the three directions in space for (111) quantum wells, since the conduction bands can become spin degenerate to first order in $\boldsymbol{k}$ [30–32]. This is possible since the BIA and SIA vectors have exactly the same direction in the QW plane and the same $\boldsymbol{k}$ dependence [Eqs. (2c) and (3), inset of Fig. 2(a)]. If the electric field amplitude E is tuned to the value,

$$\frac{2\gamma}{\sqrt{3}}\langle k_z^2 \rangle = -aE, \tag{4}$$

the DP spin relaxation should be suppressed for S_x, S_y, S_z since all components of $\boldsymbol{\Omega}$ vanish. To the best of our knowledge, this has not been evidenced experimentally.

In this Letter we have measured the electron spin relaxation time in (111) GaAs quantum wells by time-resolved photoluminescence (PL). By embedding the QWs in a PIN or NIP structure we demonstrate the tuning of the conduction band spin splitting and hence the spin relaxation time with an applied external electric field [33]. The spin quantum beats measurements under transverse magnetic field prove that the DP spin relaxation time is not only increased for the S_z spin component but also for both S_x and S_y.

We have studied three samples grown on n-doped (111)B GaAs substrates ($n = 2 \times 10^{18}$ cm^{-3}) by molecular beam epitaxy. These substrates are misoriented 3° towards $\langle 111 \rangle A$. For the three samples, the multiple quantum well (MQW) region consists of 20 GaAs/$Al_{0.3}Ga_{0.7}As$ QWs with a barrier width $L_B = 12$ nm. Samples I and II have a well width equal to $L = 15$ nm, whereas $L = 7.5$ nm for sample III. In samples I and III, these layers form a PIN device with the following structure sequence [Fig. 1(a)]: n-substrate/500 nm GaAs layer ($n = 2 \times 10^{18}$ cm^{-3})/500 nm AlGaAs

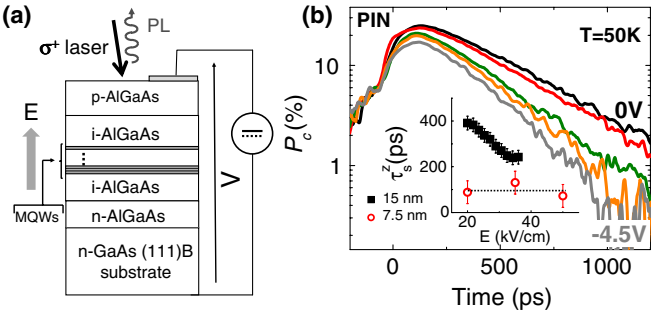

FIG. 1 (color online). (a) PIN GaAs/AlGaAs MQW structure. E is positive when it points along the growth direction. (b) Circular polarization dynamics for different reverse bias voltages V for sample I ($L = 15$ nm). Inset: Dependence of the electron spin relaxation time with the electric field for samples I and III ($L = 7.5$ nm).

($n = 2 \times 10^{18}$ cm^{-3})/100 nm nonintentionally doped (nid) AlGaAs/MQW/100 nm nid AlGaAs/500 nm p AlGaAs ($p = 2 \times 10^{18}$ cm^{-3})/5 nm p^+ GaAs ($p = 1 \times 10^{19}$ cm^{-3}). The bias is applied between the surface p contact and the substrate back n contact. In sample II, the n- and p-doped layers are reversed in the sequence and, in addition, a 500 nm nid GaAs layer followed by a 100 nm nid AlGaAs layer are grown just above the substrate. In this NIP structure, the bias is applied between the unetched top n contact and the chemically etched p contact. The built-in electric field $|E|$ in the PIN or NIP structure is about 20 kV/cm. Applying a reverse bias in these samples allows us to tune the sign and amplitude of the Rashba (SIA) spin splitting. The electric field in the MQW region is determined from measurements of the quantum confined Stark effect [34,35]. The samples are excited by circularly polarized (σ^+) 1.5 ps pulses generated by a mode-locked Ti:sapphire laser with a repetition frequency of 80 MHz (average power $P_{\text{exc}} = 10$ mW, 50 μm diameter spot). The laser excitation energy is set to 1.56 eV, i.e., above the E1-LH1 quantum well transition. The E1-HH1 transition time-resolved PL is then recorded using a S1 photocathode streak camera with an overall time resolution of 8 ps. The PL intensity of the E1-HH1 transition copolarized (I^+) and counterpolarized (I^-) with the excitation laser is then recorded and the PL circular polarization degree is defined as $P_c = (I^+ - I^-)/(I^+ + I^-)$.

Figure 1(b) displays the PL circular polarization dynamics P_c for different bias voltages V in sample I at $T = 50$ K. Let us recall that P_c probes directly the QW electron spin dynamics in these nonresonant excitation conditions [1,12] since (i) the hole spin relaxation time is very fast (of the order of $\tau_h \sim 1$ ps) and (ii) the exciton spin relaxation time due to the electron-hole exchange interaction is inefficient due to the short τ_h. We observe in Fig. 1(b) a clear variation of the electron spin relaxation time with V: the relaxation time *decreases* when the reverse bias increases, i.e., when the electrons in the quantum

wells feel a larger electric field E. This variation rules out a possible role played by the exciton spin relaxation mechanism (induced by the exchange interaction). Indeed, it was shown that the application of an external electric field when excitons are excited strictly resonantly yields an *increase* of the polarization decay time due to the reduction of the exchange interaction (weaker overlap between the electron and hole wave functions) [35]. Thus, the results in Fig. 1(b) demonstrate that the electron spin relaxation time in (111) quantum wells can be tuned by the Rashba effect. In the narrow MQW ($L = 7.5$ nm, sample III), we see in the inset of Fig. 1(b) that the electric field has almost no effect on the spin relaxation compared to the one in sample I as a consequence of the larger BIA splitting due to the stronger $\langle k_z^2 \rangle = (\pi/L)^2$ term. However, in these PIN devices, it turns out that the Dresselhaus and Rashba $\mathbf{\Omega}$ vectors have the same direction and same sign. In other words, these two contributions to the conduction band spin splitting add up: $\mathbf{\Omega}$ increases with E and the DP spin relaxation time decreases with the reverse bias.

In order to check this assumption, we have measured the electron spin dynamics in sample II where the applied electric field direction is reversed with respect to the one in sample I. In this case we expect to reduce the CB spin splitting (the BIA and SIA terms will subtract to each other) and as a consequence an *increase* of the electron spin relaxation time with the applied reverse bias should be observed. Figure 2(a) presents the variation of the electron spin dynamics with the applied reverse bias in sample II (NIP structure). A spectacular increase of the electron spin relaxation time is observed when the electric field modulus $|E|$ increases. The dependence of the electron spin relaxation time τ_s^z as a function of E is displayed in Fig. 2(b) (circles): the electron spin relaxation time increases from 500 to ~30 000 ps when $|E|$ varies from 20 to 55 kV/cm. For $|E| > 50$ kV/cm, the electron spin relaxation time ($\tau_s^z > 10$ ns) becomes much longer than the carrier lifetime so that it is difficult to measure it in time-resolved PL. For larger $|E|$ we expect that an efficient DP spin relaxation should be switched on again because the spin splitting would not be zero anymore [30]. The NIP device characteristics did not allow us to test this prediction (55 kV/cm is the maximum achievable electric field). Assuming that $E = -55$ kV/cm is close to the cancellation of the spin splitting on the basis of the very long measured τ_s^z, we can extract from Eq. (4) the ratio between the Dresselhaus γ and the Rashba α coefficients. We find $\alpha/\gamma \approx 5 \times 10^{16}$ m^{-2}. No measurements were made before in (111) QW for comparison. Nevertheless, using the measured γ value in a (001) QW with similar confinement energy ($|\gamma| = 11$ eV $\cdot$ Å^3) [36] gives a Rashba coefficient $\alpha = 550 \times 10^{-15}$ eV $\cdot$ m, which is in good agreement with the coefficient measured in a (110) MQW sample with an applied field of 60 kV/cm ($\alpha = 500 \times 10^{-15}$ eV $\cdot$ m) [37]. These results demonstrate that the electron spin relaxation time in (111) quantum wells can be tuned with an applied electric field thanks to the Rashba-induced variation of the CB spin splitting.

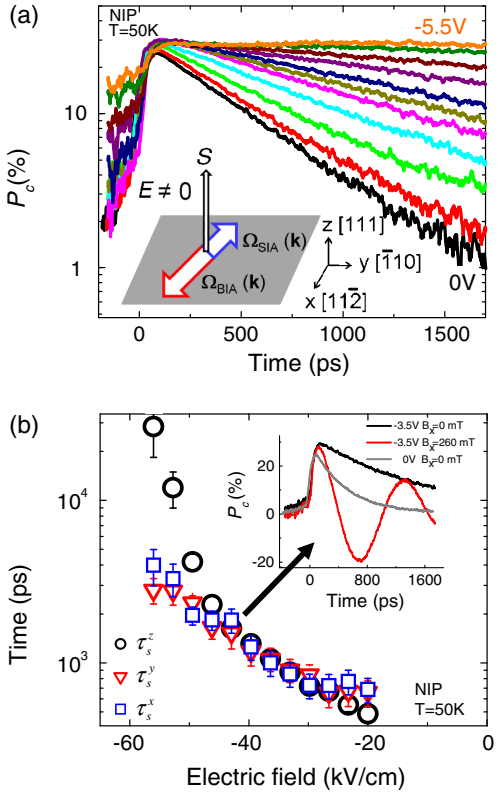

FIG. 2 (color online). Sample II (NIP). (a) Electron spin dynamics at $T = 50$ K for different reverse voltages. Inset: Schematic of the BIA ($\mathbf{\Omega_{BIA}}$) and SIA ($\mathbf{\Omega_{SIA}}$) precession vectors in (111) GaAs quantum wells. $\boldsymbol{S}$ is the photogenerated electron spin at $t = 0$. (b) Dependence of the electron spin relaxation times τ_s^z (circles), τ_s^y (triangles), τ_s^x (squares), as a function of the electric field. Inset: PL circular polarization dynamics for $B_x = 0$ and $B_x = 0.26$ T ($V = -3.5$ V, see arrow). The P_c dynamics for $V = 0$ and $B_x = 0$ is also displayed.

Nevertheless, we have shown so far that only very long electron relaxation times for spins which are oriented along the [111] growth direction can be obtained with the reverse bias in the NIP structure. We recall that in the optical spin orientation experiments presented here, the photogenerated electron spin is parallel to the growth direction, which is also the propagation direction of the excitation laser beam [inset of Fig. 2(a)]. In order to test that the relaxation time can also be controlled electrically for spins along the **x** and **y** in-plane QW direction, which is the key feature of (111) quantum wells, we have measured the electron spin dynamics in a transverse magnetic field (Voigt configuration). Following the circularly polarized laser excitation, the electron spins will be first oriented along the **z** axis but will then precess around the in-plane external magnetic field. As a consequence, the electron spins should experience both in-plane and out-of plane spin relaxation

processes. The inset of Fig. 2(b) depicts the PL circular polarization dynamics for $B_x = 0$ and $B_x = 0.26$ T in the NIP sample. In both cases, the same reverse bias $V = -3.5$ V is applied (the decay for $V = 0$ V is also displayed as a reference). For $B_x = 0$, the average electron spin direction is always oriented along the **z** direction; we measure $\tau_s^z = 1630$ ps (compared to $\tau_s^z = 490$ ps at $V = 0$ V). For $B_x = 0.26$ T, we observe the expected oscillations as a result of the electron spin Larmor precession around the external magnetic field B_x. The Larmor precession period yields the measured electron spin Landé factor $|g| = 0.22$ [38]. The striking feature here is that the circular polarization decay time in the presence of the external transverse magnetic field is almost the same as the one for $B_x = 0$. Similar results have been obtained for different B_x in the 0.26–0.7 T range. We measure a spin relaxation time $(1/\tau_s^z + 1/\tau_s^y)/2$ which yields $\tau_s^y = 1530 \pm 300$ ps. We have performed the same experiment for an applied magnetic field along the **y** direction, which gives $\tau_s^x = 1830 \pm 300$ ps.

The large increase of τ_s^x and τ_s^y observed as a function of $|E|$ [see Fig. 2(b)] demonstrates that the DP spin relaxation time in (111) quantum wells can not only be controlled electrically for the S_z electron spin component but also for both S_x and S_y. These results contrast drastically with the (001) and (110) quantum wells [22–24,27,29].

Nevertheless, we observe in Fig. 2(b) that the in-plane spin relaxation times are shorter than the out-of plane ones for the large applied electric fields ($|E| \geq 50$ kV/cm). When both Rashba and Dresselhaus terms have similar amplitudes at a nonzero temperature, we believe that the main reason for a large spin relaxation anisotropy is due to the cubic Dresselhaus term which has been neglected in Eq. (2c). Taking into account this nonlinear term, the total CB spin splitting is determined by [30–32]:

$$\begin{aligned}\boldsymbol{\Omega} &= \boldsymbol{\Omega}_{\mathrm{BIA}} + \boldsymbol{\Omega}_{\mathrm{SIA}} \\ &\equiv \begin{cases} \Omega_x(\boldsymbol{k}_\parallel) = \frac{1}{\hbar}\left[\frac{\gamma}{\sqrt{3}}\left(2\langle k_z^2\rangle - \frac{k_\parallel^2}{2}\right) + aE\right]k_y \\ \Omega_y(\boldsymbol{k}_\parallel) = -\frac{1}{\hbar}\left[\frac{\gamma}{\sqrt{3}}\left(2\langle k_z^2\rangle - \frac{k_\parallel^2}{2}\right) + aE\right]k_x \\ \Omega_z(\boldsymbol{k}_\parallel) = \frac{1}{\hbar}\left(\frac{3k_x^2k_y - k_y^3}{\sqrt{6}}\right). \end{cases} \end{aligned} \tag{5}$$

This equation shows that for a given $\boldsymbol{k}$ the strict compensation of the Rashba and Dresselhaus terms can only occur for the in-plane components Ω_x and Ω_y. As a consequence, electron spins oriented along the **z** axis will have longer spin relaxation times compared to the ones oriented in the plane since the latter will precess around a nonzero vector $\boldsymbol{\Omega}$, which is orthogonal to the QW plane [32]. Moreover Eq. (5) demonstrates that the compensation cannot strictly occur simultaneously for a large range of electron wave vectors. When the temperature increases, higher k states are populated where the cubic Dresselhaus term plays a larger role [31]. Despite this nonlinear Dresselhaus term, we observed a clear control of the SO spin splitting in the 15 nm MQW at high temperature. A factor of 5 increase of the spin relaxation time τ_s^z is still observed when the bias varies from 0 to -3 V at $T = 150$ K (close to the ratio observed at $T = 50$ K). Above 150 K, it was not possible to separate the Stark-shifted QW and the bulk GaAs luminescence, which prevented us from getting room temperature data. For larger quantum wells at high temperature, one also has to consider other spin relaxation mechanisms due to the scattering of electrons between different QW subbands [27,39]. We emphasize that the tuning or suppression of the DP electron spin relaxation demonstrated here for GaAs/AlGaAs quantum wells is also possible in many other III-V and II-VI zinc-blende nanostructures since the principle relies only on symmetry considerations. Spin transport of electrons over long distances even at elevated temperature could, in principle, be demonstrated using these (111) engineered QW [40–42]. The control of the built-in piezoelectric field in a strained (111) InGaAs quantum well could also permit one to reduce significantly the DP spin relaxation even in the absence of an applied external field. This would open new perspectives for spin manipulation and control in solid state systems.

This work was supported by the France-China NSFC-ANR research project SPINMAN (Grant No. 10911130356) and CAS Grant No. 2011T1J37; we thank H. Carrère and M. W. Wu for useful discussions and S. Pinaud, G. Almuneau, and A. Arnoult for technical support.

*marie@insa-toulouse.fr

[1] F. Meier and B. P. Zakharchenya, *Optical Orientation* (Elsevier Science Ltd., New York, 1984).
[2] D. Awschalom, D. Loss, and N. Samarth, *Semiconductor Spintronics and Quantum Computation* (Springer, New York, 2002).
[3] M. Dyakonov, *Spin Physics in Semiconductors* (Springer, New York, 2008).
[4] M. I. D'yakonov and V. I. Perel', Fiz. Tverd. Tela **13**, 3581 (1971)[Sov. Phys. Solid State **13**, 3023 (1972)].
[5] M. I. D'yakonov and V. Yu. Kachorovskii, Fiz. Tekh. Poluprovodn. **20**, 178 (1986)[Sov. Phys. Semiconductors **20**, 110 (1986)].
[6] I. Žutić, J. Fabian, and S. Das Sarma, Rev. Mod. Phys. **76**, 323 (2004).
[7] E. L. Ivchenko, *Optical Spectroscopy of Semiconductor Nanostructures* (Alpha Science International, Ltd., Harrow, 2005).
[8] G. Dresselhaus, Phys. Rev. **100**, 580 (1955).
[9] Y. A. Bychkov and E. I. Rashba, J. Phys. C **17**, 6039 (1984).
[10] O. Krebs and P. Voisin, Phys. Rev. Lett. **77**, 1829 (1996).
[11] A. Malinowski *et al.*, Phys. Rev. B **62**, 13034 (2000).
[12] T. Amand *et al.*, Phys. Rev. Lett. **78**, 1355 (1997).
[13] J. H. Buß *et al.*, Appl. Phys. Lett. **97**, 062101 (2010).
[14] D. Lagarde *et al.*, Phys. Rev. B **77**, 041304 (2008).

[15] N. S. Averkiev and L. E. Golub, Phys. Rev. B **60**, 15582 (1999).
[16] J. Kainz, U. Rossler, and R. Winkler, Phys. Rev. B **68**, 075322 (2003).
[17] J. B. Miller *et al.*, Phys. Rev. Lett. **90**, 076807 (2003).
[18] P. S. Eldridge *et al.*, Phys. Rev. B **83**, 041301 (2011).
[19] B. Jusserand *et al.*, Phys. Rev. B **51**, 4707 (1995).
[20] J. Schliemann, J. C. Egues, and D. Loss, Phys. Rev. Lett. **90**, 146801 (2003).
[21] V. Lechner *et al.*, Appl. Phys. Lett. **94**, 242109 (2009).
[22] D. Stich *et al.*, Phys. Rev. B **76**, 073309 (2007).
[23] N. S. Averkiev *et al.*, Phys. Rev. B **74**, 033305 (2006).
[24] B. Liu *et al.*, Appl. Phys. Lett. **90**, 112111 (2007).
[25] J. D. Koralek *et al.*, Nature (London) **458**, 610 (2009).
[26] Y. Ohno *et al.*, Phys. Rev. Lett. **83**, 4196 (1999).
[27] S. Döhrmann *et al.*, Phys. Rev. Lett. **93**, 147405 (2004).
[28] W. H. Lau and M. E. Flatté, J. Appl. Phys. **91**, 8682 (2002).
[29] O. Z. Karimov *et al.*, Phys. Rev. Lett. **91**, 246601 (2003).
[30] X. Cartoixà, D. Z.-Y. Ting, and Y. C. Chang, Phys. Rev. B **71**, 045313 (2005).
[31] I. Vurgaftman and J. R. Meyer, J. Appl. Phys. **97**, 053707 (2005).
[32] B. Y. Sun *et al.*, J. Appl. Phys. **108**, 093709 (2010).
[33] PIN (NIP) stands for a positively (negatively) doped-intrinsic-negatively (positively) doped structure starting from the top to the bottom of the sample.
[34] R. L. Tober and T. B. Bahder, Appl. Phys. Lett. **63**, 2369 (1993).
[35] A. Vinattieri *et al.*, Appl. Phys. Lett. **63**, 3164 (1993).
[36] W. J. H. Leyland *et al.*, Phys. Rev. B **76**, 195305 (2007).
[37] P. S. Eldridge *et al.*, Phys. Rev. B **77**, 125344 (2008).
[38] We observe a negligible variation of the g factor when E increases. A weak $\Delta g/g$ has been measured (not shown) but here it plays a negligible role in the damping of the oscillations.
[39] E. Bernardes *et al.*, Phys. Rev. Lett. **99**, 076603 (2007).
[40] J. M. Kikkawa and D. D. Awschalom, Nature (London) **397**, 139 (1999).
[41] O. D. D. Couto *et al.*, Phys. Rev. Lett. **98**, 036603 (2007).
[42] C. Hu *et al.*, Nano. Res. Lett. **6**, 149 (2011).